Desalination and Water Treatment
www.deswater.com

doi: 10.5004/dwt.2017.21233

90 (2017) 189–195
September

A facile synthetic method of ZnO nanoparticles and its role in photocatalytic degradation of refractory organic matters

Hanbing Zhang[a,b], Zhenyu Song[c], Dingyong Wang[a,*], Zhangfa Tong[c], Yuelong Qin[b]

[a]*College of Resources and Environment, Southwest University, Chongqing 400715, China, Tel. +86 2368251691, emails: dywang@swu.edu.cn (D. Wang), coldicezhang0771@163.com (H. Zhang)*
[b]*School of Environment, Guangxi University, Nanning 530004, China, email: 362666493@qq.com (Y. Qin)*
[c]*Guangxi Key Laboratory of Petrochemical Resource Processing and Process Intensification Technology, School of Chemistry and Chemical Engineering, Guangxi University, Nanning 530004, Guangxi, China, emails: 506390461@qq.com (Z. Song), zhftong@sina.com (Z. Tong)*

Received 16 November 2016; Accepted 16 July 2017

ABSTRACT

Treatment of refractory organic dyeing wastewater is a serious issue in the chemical industry and environmental protection. ZnO nanomaterials have a good potential for dyes removal from wastewater. To optimize the synthetic technology for ZnO and improve the photocatalytic activity for hazardous organic matters, an improved route of ZnO were proposed via microwave-assisted co-precipitation method using polyethylene glycol 400 (PEG 400) as a surfactant. The facile and moderate synthesis conditions of ZnO nanoparticles (NPs) were confirmed owing to lower reaction temperature (35°C) and quick reaction time (5 min microwave irradiation). The as-prepared ZnO NPs exhibited excellent photocatalytic degradation performance for refractory dyes crystal violet (CV) and Congo red (CR) in terms of rapid degradation rate, high degradation efficiency and broad pH range. In summary, the study is very useful for optimizing the synthetic conditions for the ZnO NPs and enhancing the potential applications in photocatalytic degradation for refractory organic pollutants.

Keywords: ZnO nanoparticles; Microwave radiation; Crystal violet; Congo red; Photocatalytic degradation

1. Introduction

Many industries such as textiles, paper and other coloring industries usually produce large volumes of wastewater containing organic dyes. These dyes in wastewater are hazardous in terms of their mutagenic as well as carcinogenic effect, which easily induce damage to aquatic ecosystem and humans [1]. Photocatalytic degradation is considered as the promising method for disposal of wastewater containing dyes due to its ability of decomposing hazardous organic dyes into less harmful matters.

In recent years, ZnO semiconductor nanomaterial has attracted considerable attention owing to its properties such as stability, low cost and good photocatalytic performance for different types of dyes. Commonly used methods for the ZnO NPs synthesis include chemical precipitation method, hydrothermal method, solvothermal method and sol–gel method. However, the abovementioned methods usually suffer from many disadvantages such as long reaction time, high reaction temperature, high pressure or use of toxic surfactants [2,3]. While microwave heating is well known for its numerous advantages including energy saving, fast reaction rate and homogeneity [4,5]. Moreover, previous studies have revealed that surfactants considered as both a solvent and a dispersant could greatly influence the properties of ZnO nanomaterials [6,7]. Among various surfactants, polyethylene glycol 400 (PEG 400) is found to be inexpensive, environment-friendly and easily soluble. Being a nonionic surfactant containing a large number of OH groups, in one hand, PEG 400 can enhance the dispersion of ions in reaction system due to steric hindrance effect. Hence, it helps to adjust

* Corresponding author.

the morphologies and defects of nanomaterials availably. On the other hand, PEG 400 is an ideal solvent for the microwave heating. PEG 400 can improve the efficiency of microwave heating due to its relatively high dielectric constant and a high boiling point of 250°C. Wang et al. [8] synthesized the flower-like ZnO microstructures via hydrothermal method using PEG 4000 as adjusting agent to control the morphology and structure of ZnO. Limited work has been conducted on organic compounds synthesis using PEG coupled with microwave heating. Ganapathi et al. [9] reported the efficient synthesis of diphenyl substituted pyrazole using PEG 600 as solvent assisted with microwave heating. However, the related work on nanomaterials synthesis using PEG via microwave assist is not well explored yet.

Meanwhile, it is limited to the few dyes as model pollutants for evaluating ZnO photocatalytic degradation performance, such as methylene blue, methyl orange and rhodamine B [10,11]. Crystal violet (CV) and Congo red (CR) are the representative cationic and anionic dyes, respectively. Both CV and CR are detrimental to health especially at elevated concentrations, causing irritation of the respiratory tracts, gastrointestinal tracts and inducing some neurologic disorders [12,13]. To date, it is relatively insufficient for the reports on cation dye CV or anion dye CR degradation by the ZnO NPs [14,15].

Hence, there is still enough research potential to focus on optimizing the synthetic conditions for the ZnO NPs including shorten reaction time and reduced reaction temperature to improve the photocatalytic degradation capability. To the best of our knowledge, a synthesis of ZnO nanomaterial using PEG as a surfactant under microwave irradiation condition has not been reported so far. In this work, we proposed a quicker and moderate approach for the ZnO NPs synthesis using PEG 400 as a solvent and dispersant via microwave heating. Furthermore, the obtained ZnO sample exhibited good photocatalytic degradation performance for either cation dyes or anionic ones as shown by its excellent photocatalytic performance on CV and CR.

2. Experimental

2.1. Synthesis of the ZnO NPs

The typical synthesis of the ZnO NPs is as follows: first, $Zn(NO_3)_2 \bullet 6H_2O$ (0.025 mol) was dissolved in 25 mL PEG 400 in order to achieve better dispersion. NaOH (0.05 mol) and 25 mL PEG 400 were mixed in 40 mL deionized water. Then, the above two solutions were then dispersed separately under sonication for 10 min. NaOH solution was slowly dripped to $Zn(NO_3)_2 \bullet 6H_2O$ solution under constant stirring for 30 min to obtain the homogeneous suspension. Thereafter, the resultant mixture was heated at 35°C for 5 min in a microwave oven with magnetic stirring. Afterward, the obtained white precipitates were washed several times by deionized water and ethanol. The final products were calcined at 350°C for 2 h to obtain the ZnO NPs. The schematic diagram for the ZnO NPs synthesis was shown in Fig. 1.

2.2. Photocatalytic experiments

For the evaluation of the photocatalytic degradation capability of obtained material, 0.2 and 0.5 g L^{-1} ZnO were added to 50 mg L^{-1} CV solution and CR solution, respectively. The solutions were continuously stirred for 30 min under dark condition in order to attain the adsorption–desorption equilibrium between dyes and ZnO. The photocatalytic degradation of CV and CR was carried out under UV-light illumination using mercury arc lamp (300 W). The sampled suspensions were centrifuged at 6,000 rpm and then the supernatants were analyzed by UV–Vis spectrophotometer (2550-Shimadzu, Japan). The respective determining wavelengths of CV and CR are 585 and 497 nm, respectively. The degradation efficiency (%) of CV and CR was evaluated by the following Eq. (1):

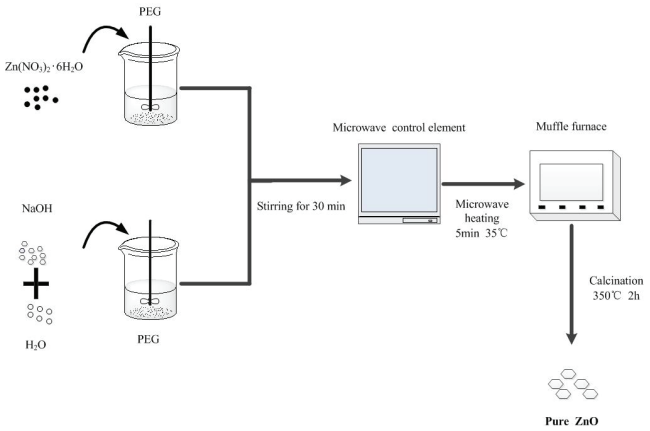

Fig. 1. The schematic diagram for the ZnO NPs synthesis.

$$\text{Degradation efficiency}\ (\%) = \frac{C_0 - C}{C} \times 100\% \quad (1)$$

where C_0 and C are the initial concentration and the concentration at any time t of the dyes, respectively.

3. Results and discussion

3.1. Material characterizations of the ZnO NPs

The morphology of the ZnO NPs was observed by field emission scanning electron microscope (FESEM, Hitachi SU-8020, Japan), various shapes and sizes of the ZnO NPs can be seen from the FESEM image (Fig. 2(a)). The ZnO NPs had non-uniform size with an average diameter of 52 nm in length. The longest and shortest diameters of the ZnO NPs were about 129 and 16 nm, respectively. The ZnO NPs might be aggregated to some extent since there were many smaller particles on bigger ones. In addition, the aggregation state of the ZnO NPs needs to be analyzed by high resolution transmission electron microscope (HRTEM) in further study. The ZnO aggregates may produce smaller or larger surface-to-volume ratio, which was important for dye molecules adsorption on catalysts and consequently affected the photocatalytic performance.

The diffraction peaks of the ZnO NPs were identified using X-ray diffractomer (XRD; Fig. 2(b)). The main XRD instrument conditions were set as follows the respective working voltage and acceleration current of XRD instrument were 40 kV and 20 mA and the radiation source was Cu/Kα (λ = 0.154 nm) from 2θ = 10°–80° with a step size of 0.02°and

dwell time of 0.5° min^{-1}. The XRD data were analyzed using Materials Data (MDI) Jade 2010 analytical software. Fig. 2(b) indicated that all the diffraction peaks of the ZnO NPs were well-indexed to JCPDS No. 36-1451, confirming the typical hexagonal wurtzite structure of the obtained ZnO sample [16]. Furthermore, the relatively sharp diffraction peaks and no other peaks related to impurities in the patterns indicated the well-crystallinity and purity of the ZnO NPs.

Fourier transform infrared spectroscopy (FTIR) spectrum of the ZnO NPs was shown in Fig. 3(a). The peaks around 400 and 1,450 cm^{-1} represented ZnO characteristic phase and stretching vibration, respectively [17,18]. The respective peaks at 3,419 and 1,640 cm^{-1} corresponded to OH stretching vibration and H–O–H bending vibration, indicating that small amount of water is present in the ZnO NPs [19]. The peaks between 600 and 881 cm^{-1} appeared because of the stretching vibrations of ZnO bonds [20]. There were no C–O stretching vibration peaks between 1,300 and 1,000 cm^{-1}, in FTIR spectrum, hence, PEG had been removed during the calcination process.

The UV–Vis diffuse reflectance spectrum (UV-DRS) of the ZnO NPs was presented in Fig. 3(b). The ZnO NPs exhibited strong absorption in the ultraviolet region with an adsorption sharp edge near 400 nm, corresponding to the direct band gap of bulk ZnO with hexagonal wurtzite structure [21]. Meanwhile, the ZnO NPs had weak absorption in the visible region of 400–800 nm. The estimated band gap from the UV-DRS spectrum was ~3.28 eV, which was close to the band gap of ZnO reported previously [22]. Hence, it is concluded that the ZnO NPs have better photocatalytic degradation performance under UV light irradiation compared with visible light irradiation.

The specific surface area and pore size distribution of ZnO were determined using nitrogen adsorption apparatus (TristarII 3020, USA). Pore volume (V_t) and pore size (D) were calculated by using the Barrett–Joyner–Halenda model. The Brunauer–Emmett–Teller surface area of ZnO was 9.2 $m^2 g^{-1}$, so there might be the aggregation state of the ZnO NPs. As can be seen in Fig. 4, the pore volume was calculated with the relative pressure p/p_0 = 0.99 and the ZnO nitrogen adsorption–desorption isotherm exhibited a Type-III hysteresis loop. Therefore, the ZnO NPs exhibited the characteristics of mesoporous materials. In addition, the pore sizes of the ZnO NPs were in the range of 2 to 50 nm. Therefore, the ZnO NPs had efficient dye access channels for adsorption.

3.2. Comparison of the ZnO NPs by different methods

The reported synthesis methods of the ZnO NPs were compared with the present work in Table 1 [5–7,16,18,23,24]. Compared with the traditional methods of the ZnO NPs synthesis, the aid of microwave irradiation in literature [4,25] and present work can shorten the reaction time of the ZnO NPs, which again confirmed the advantages of microwave-assisted heating resulting in fast reaction kinetics and homogeneity. Furthermore, PEG 400 can act as a good medium to absorb and transfer microwave energy to the reactants, so it can facilitate to cross energy barriers and accelerate the formation of the ZnO NPs [26]. Therefore, this synthesis method introduced with PEG 400 and microwave heating is competitive with those listed in other literature. The as-formed ZnO NPs were calcined at 350°C for 2 h to

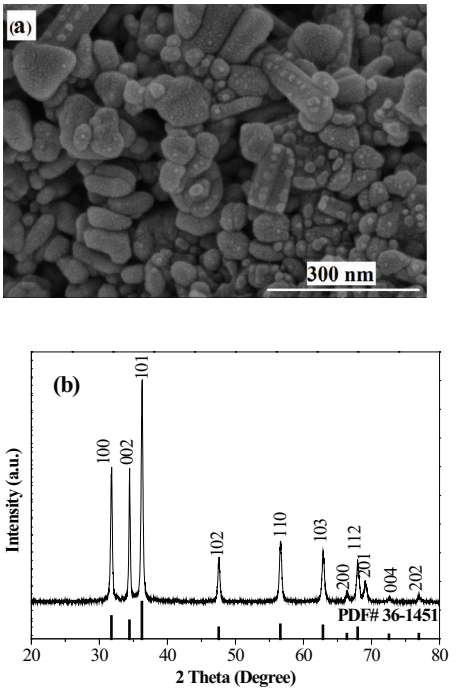

Fig. 2. (a) FESEM image and (b) XRD patterns of the ZnO NPs.

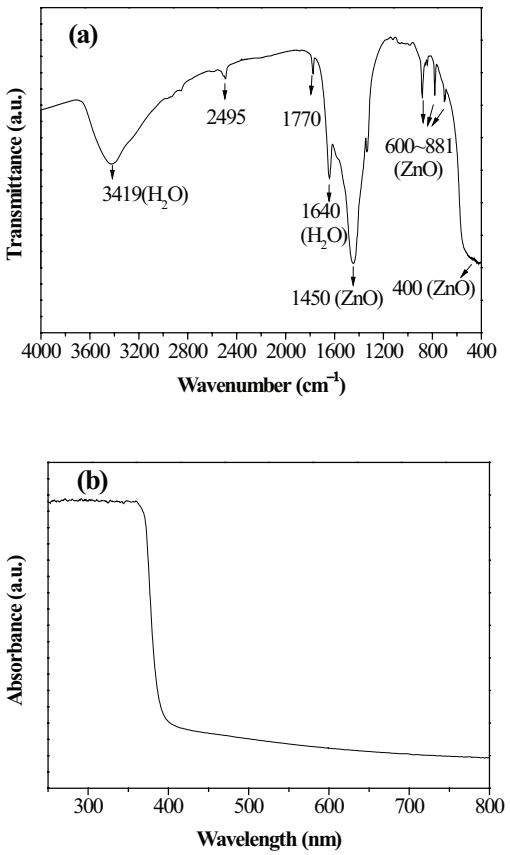

Fig. 3. (a) FTIR spectrum and (b) UV-DRS spectrum of the ZnO NPs.

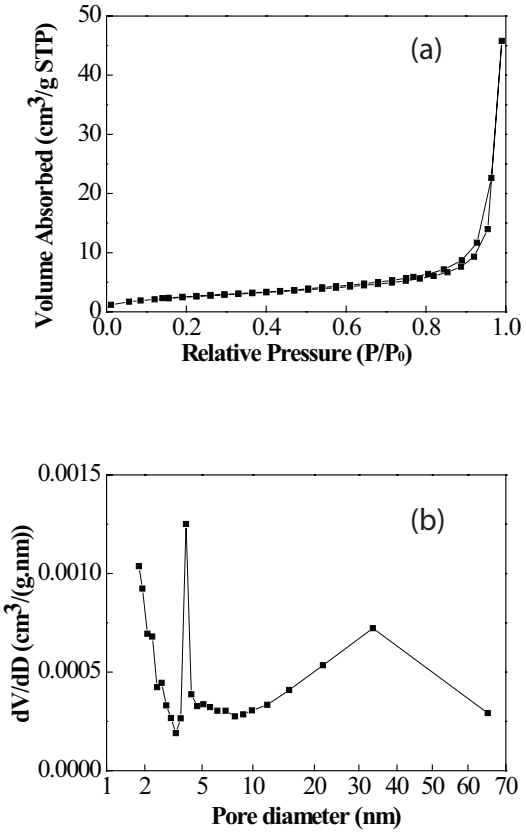

Fig. 4. (a) N_2 adsorption–desorption isotherm and (b) pore size distribution of the ZnO NPs.

remove impurities (primarily PEG), which was similar with the calcination conditions of other ZnO nanomaterials.

3.3. Photocatalytic activities of the ZnO NPs

Two typical dyes, a cationic dye CV and an anionic dye CR, were selected as target pollutants to evaluate the photocatalytic performance of the as-prepared ZnO NPs under UV light (Hg-lamp) irradiation. Fig. 5 shows the respective absorption spectra changes of CV and CR solutions under UV light irradiation using the as-prepared ZnO NPs. The characteristic absorption peaks of both CV (~585 nm) and CR (~497 nm) decreased with increasing irradiation time. After 120 min of UV light irradiation, the characteristic absorption peaks of CV and CR at their respective maximum absorption wavelengths almost completely disappeared, suggesting the dramatic decrease of CV and CR concentrations.

Fig. 6 shows photocatalytic degradation efficiency vs. time interval plots for CV and CR, which further confirmed effective degradation of the two selected dyes by the ZnO NPs again. Clearly, the photocatalytic degradation rate of CV was significantly faster than that of CR, reaching ~95% removal within 60 min. While for CR, on the other hand, the degradation efficiency reached ~60% within 60 min and asymptotically approached 95% over the duration of the experiment. Basing on the pseudo-first-order kinetic equation, the calculated kinetic rate constants of the ZnO NPs were 0.0529 min^{-1} for CV degradation and 0.0186 min^{-1} for CR degradation. The pseudo-first-order kinetic rate values of the ZnO NPs for CV and CR were compared with those of other catalysts from literature in Table 2 [27–30]. It can be seen that

Table 1
Comparison of the ZnO NPs by different methods under various conditions

Method	Precursors	Reaction condition	Drying or calcination condition	Ref.
Co-precipitation method assisted with microwave radiation	$Zn(CH_3COO)_2.2H_2O$ + NaOH + DMF	300 W microwave radiation, 1 h	Dried in a vacuum at 60°C for 4 h + annealed at 500°C	[5]
Sol–gel method	$Zn(CH_3COO)_2.2H_2O$ + C_2H_5OH + NaOH	35°C, 3 h	Dried at 60°C for 1 h	[6]
Solvothermal method	Zinc acetate + PEG-400 (or PEG 200 or EG	170°C–180°C, 2 h	Dried at 70°C for 15–20 min	[7]
Co-precipitation method	$Zn(CH_3COO)_2.2H_2O$ + $NH_3.H_2O$	90°C, 12 h	Dried at 60°C for overnight	[16]
Co-precipitation method	$Zn(CH_3COO)_2.2H_2O$ + NH_4HCO_3	Room temperature, 2 h	Dried at 80°C for overnight + calcined at 300°C for 2 h	[18]
Hydrothermal method assisted with microwave radiation	$Zn(CH_3COO)_2.2H_2O$ + NaOH	Microwave radiation at 95°C for 10 min, 20 min or 30 min	Dried at 60°C for 24 h + calcined at 500°C for 2 h.	[23]
Solvothermal method	$Zn(CH_3COO)_2$ + DMA_C	95°C, 3 h	Dried at 80°C for overnight	[24]
Co-precipitation method assisted with microwave radiation	$Zn(NO_3)_2.6H_2O$ + NaOH + PEG 400	Microwave radiation at 35°C for 5 min	Calcined at 350°C for 2 h	Present work

the ZnO NPs had quick photocatalytic activity towards CV and CR in present work.

Because ZnO is a typical amphoteric compound, the experiment about effect of initial pH on the photocatalytic degradation of CV and CR was conducted within the relatively neutral pH range 5–10. Fig. 7 shows that photocatalytic degradation efficiency of the ZnO NPs was affected to some extent by variation in initial pH of dyes solution. For CV, there was a gradual increase in photocatalytic degradation efficiency with pH increase from 5 to 8. Maximum CV degradation (about 99%) by the ZnO NPs was obtained in the pH range of 8–10 with negligible difference. For CR, there were insignificant increases/decreases in photocatalytic degradation with increasing pH from 5 to 10. The observations can be explained on both the properties of dye molecule and the changes of surface functional groups of ZnO at different initial pH. In one hand, CV and CR are cationic and anionic, respectively. As initial pH increased, more negatively charged surface sites of the ZnO NPs became available thus facilitating greater CV adsorption and photocatalytic degradation compared with CR [27]. On the other hand, it is better to produce high concentration of free hydroxyl radicals from reaction between holes (h^+) in the valance band and OH groups at higher pH values. As a result, the photocatalytic activity of ZnO semiconductor for dyes is further enhanced with increasing pH [31]. Generally, CR degradation efficiency remained ~80% within the pH range of the experiments. It was noteworthy that the degradation efficiency for CV was notably higher than for CR throughout the pH range. The results indicated that CV can more easily degraded by the ZnO NPs compared with CR.

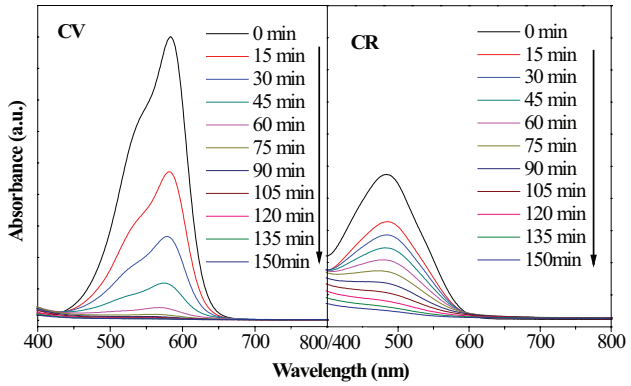

Fig. 5. The UV–Vis absorbance spectra of CV and CR degradation by the ZnO NPs.

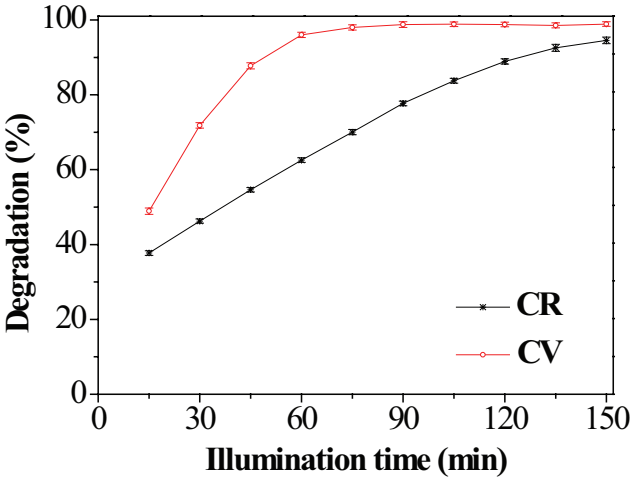

Fig. 6. Effect of illumination time on the photocatalytic degradation of CV and CR.

Table 2
Comparison of the pseudo-first-order kinetic rate constants of various photocatalysts for CV and CR degradation

Dyes	Nanomaterials	K (min^{-1})	R^2	Ref.
CV	Cu(3%)-doped ZnO	0.0394	0.9807	[27]
CV	0.8 mol% Ce–TiO_2	0.0140	0.9900	[28]
CV	ZnO	0.0529	0.9857	Present work
CR	ZnO	0.0050	0.8650	[29]
CR	1.0 g TiO_2 + UV + O2	0.0047	0.9767	[30]
CR	ZnO	0.0186	0.9734	Present work

The photocatalytic performance of the ZnO NPs for CV and CR was compared with other various photocatalysts reported in literature [27,29,32–37] (Table 3), which suggested that the ZnO materials had competitive photocatalytic activity of refractory dyes in the present work. The good photocatalytic performance of the ZnO aggregates could be related to the unique porous structure and structural defects, which needs to be determined by HRTEM and photoluminescence spectrum [18,38]. Since there are many factors related to the photocatalytic capacity, the enhanced photocatalytic activity mechanism has not been entirely investigated. Our future study will be attached to this problem.

4. Conclusions

A co-precipitation method using surfactant PEG 400 under microwave irradiation has been developed to prepare the ZnO NPs under relatively rapid and moderate conditions. The respective reaction time and reaction temperature

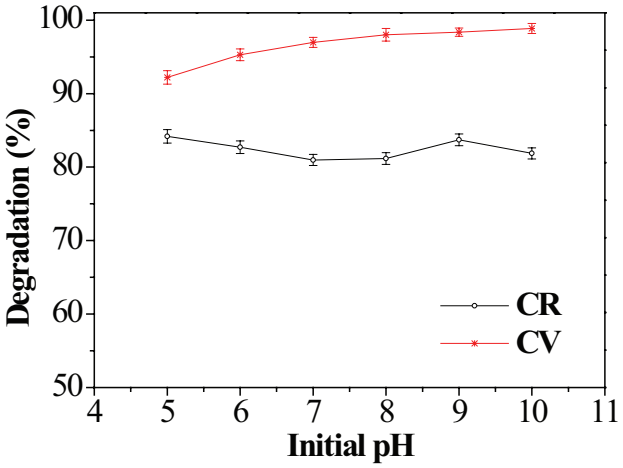

Fig. 7. Effect of initial pH on the photocatalytic degradation of CV and CR.

Table 3
Comparison of the photocatalytic performance of various photocatalysts for CV and CR degradation

Dyes	Photocatalysts	Photocatalytic time (min)	Catalyst dosage (g L^{-1})	Initial concentration of dye (mg L^{-1})	Degradation (%)	Ref.
CV	Cu(3%)-doped ZnO	210	2.5	10	96	[27]
CV	cellulose/PVC/ZnO	90	0.6	3	90	[32]
CV	TiO_2 (P25)	80	4	10.2	70.3	[33]
CV	Nitrogen-rich graphitic carbon nitride (Ng-C3N4)	135	0.25	10	87	[34]
CV	CdS	50	0.35	15	44	[35]
CV	ZnO	90	0.2	50	99	Present work
CR	ZnO	120	0.5	10	50	[29]
CR	Cellulose/PVC/ZnO	120	0.6	3	90	[32]
CR	TiO_2	60	2	50	90	[36]
CR	CdS-1	60	0.5	50	93	[37]
CR	CdS-2	30	0.5	50	95	[37]
CR	ZnO	150 (120)	0.5	50	95 (88)	Present work

were reduced to 5 min and 35°C. The irregularly shaped ZnO NPs showed a typical hexagonal wurtzite structure with an average diameter of 52 nm in length. The photocatalytic experiments confirmed that the ZnO NPs exhibited higher photocatalytic activity of CV and CR (especially for CV) degradation in terms of good degradation efficiency and broad pH range. Therefore, this study will be useful in finding improved methods for ZnO NPs synthesis and treating wastewater containing dyes.

Acknowledgments

This work was supported by the National Natural Science Foundation of China (21576055) and the Postdoctoral Research Project of Southwest University (104240-20730889).

References

[1] H. Chaudhuri, S. Dash, S. Ghorai, S. Pal, A. Sarkar, SBA-16: application for the removal of neutral, cationic, and anionic dyes from aqueous medium, J. Environ. Chem. Eng., 4 (2016) 157–166.
[2] R. Triboulet, Growth of ZnO bulk crystals: a review, Prog. Cryst. Growth Charact. Mater., 60 (2014) 1–14.
[3] I. Udom, M.K. Ram, E.K. Stefanakos, A.F. Hepp, D.Y. Goswami, One dimensional-ZnO nanostructures: synthesis, properties and environmental applications, Mat. Sci. Semicon. Proc., 16 (2013) 2070–2083.
[4] K. Ocakoglu, S.A. Mansour, S. Yildirimcan, A.A. Al-Ghamdi, F. El-Tantawy, F. Yakuphanoglu, Microwave-assisted hydrothermal synthesis and characterization of ZnO nanorods, Spectrochim. Acta, 148 (2015) 362–368.
[5] V. Kumar, M. Gohain, S. Som, V. Kumar, B.C.B. Bezuindenhoudt, H.C. Swart, Microwave assisted synthesis of ZnO nanoparticles for lighting and dye removal application, Physica B, 480 (2016) 36–41.
[6] J. Ungula, B.F. Dejene, Effect of solvent medium on the structural, morphological and optical properties of ZnO nanoparticles synthesized by the sol–gel method, Physica B, 480 (2016) 26–30.
[7] P. Srinivasan, B. Subramanian, Y. Djaoued, J. Robichaud, T. Sharma, R. Bruning, Facile synthesis of mesoporous nanocrystalline ZnO bipyramids and spheres: characterization, and photocatalytic activity, Mater. Chem. Phys., 155 (2015) 162–170.
[8] F. Wang, X. Qin, D. Zhu, Y. Meng, L. Yang, Y. Ming, PEG-assisted hydrothermal synthesis and photoluminescence of flower-like ZnO microstructures, Mater. Lett., 117 (2014) 131–133.
[9] M. Ganapathi, D. Jayaseelan, S. Guhanathan, Microwave assisted efficient synthesis of diphenyl substituted pyrazoles using PEG-600 as solvent - a green approach, Ecotoxicol. Environ. Saf., 121 (2015) 87–92.
[10] S.V. Nipane, P.V. Korake, G.S. Gokavi, Graphene-zinc oxide nanorod nanocomposite as photocatalyst for enhanced degradation of dyes under UV light irradiation, Ceram. Int., 41 (2015) 4549–4557.
[11] G.M. Neelgund, A. Oki, Z. Luo, ZnO and cobalt phthalocyanine hybridized graphene: efficient photocatalysts for degradation of rhodamine B, J. Colloid Interf. Sci., 430 (2014) 257–264.
[12] C.C. Hsueh, B.Y. Chen, Comparative study on reaction selectivity of azo dye decolorization by *Pseudomonas luteola*, J. Hazard. Mater., 141 (2007) 842–849.
[13] C. Belpaire, T. Reyns, C. Geeraerts, J.V. Loco, Toxic textile dyes accumulate in wild European eel *Anguilla anguilla*, Chemosphere, 138 (2015) 784–791.
[14] S. Ameen, M.S. Akhtar, M. Nazim, H.S. Shin, Rapid photocatalytic degradation of crystal violet dye over ZnO flower nanomaterials, Mater. Lett., 96 (2013) 228–232.
[15] N.H.H. Hairom, A.W. Mohammad, A.A.H. Kadhum, Influence of zinc oxide nanoparticles in the nanofiltration of hazardous Congo red dyes, Chem. Eng. J., 260 (2015) 907–915.
[16] H.K. Seo, H.S. Shin, Study on photocatalytic activity of ZnO nanodisks for the degradation of rhodamine B dye, Mater. Lett., 159 (2015) 265–268.
[17] K. Buvaneswari, R. Karthiga, B. Kavitha, M. Rajarajan, A. Suganthi, Effect of $FeWO_4$ doping on the photocatalytic activity of ZnO under visible light irradiation, Appl. Surf. Sci., 356 (2015) 333–340.
[18] F. Fan, Y. Feng, P. Tang, D. Li, Facile synthesis and photocatalytic performance of ZnO nanoparticles self-assembled spherical aggregates, Mater. Lett., 158 (2015) 290–294.
[19] Z.J. Yu, M. R. Kumar, D.L. Sun, L.T. Wang, R.Y. Hong, Large scale production of hexagonal ZnO nanoparticles using PVP as a surfactant, Mater. Lett., 166 (2016) 284–287.
[20] S. Yusan, A. Bampaiti, S. Aytas, S. Erenturk, M.A.A. Aslani, Synthesis and structural properties of ZnO and diatomite-supported ZnO nanostructures, Ceram. Int., 42 (2016) 2158–2163.

[21] M. Aslam, I.M.I. Ismail, T. Almeelbi, N. Salah, S. Chandrasekaran, A. Hameed, Enhanced photocatalytic activity of V_2O_5–ZnO composites for the mineralization of nitrophenols, Chemosphere, 117 (2014) 115–123.
[22] N. Huang, J. Shu, Z. Wang, M. Chen, C. Ren, W. Zhang, One-step pyrolytic synthesis of ZnO nanorods with enhanced photocatalytic activity and high photostability under visible light and UV light irradiation, J. Alloys Compd., 648 (2015) 919–929.
[23] Y. Caglar, K. Gorgun, S. Aksoy, Effect of deposition parameters on the structural properties of ZnO nanopowders prepared by microwave-assisted hydrothermal synthesis, Spectrochim. Acta, 138 (2015) 617–622.
[24] W. Feng, P. Huang, B. Wang, C. Wang, W. Wang, T. Wang, S. Chen, R. Lv, Y. Qin, J. Ma, Solvothermal synthesis of ZnO with different morphologies in dimethylacetamide media, Ceram. Int., 42 (2016) 2250–2256.
[25] W. Promnopas, T. Thongtem, S. Thongtem, Effect of microwave power on energy gap of ZnO nanoparticles synthesized by microwaving through aqueous solutions, Superlattice. Microst., 78 (2015) 71–78.
[26] K.D. Bhatte, D.N. Sawant, R.A. Watile, B.M. Bhanage, A rapid, one step microwave assisted synthesis of nanosize zinc oxide, Mater. Lett., 69 (2012) 66–68.
[27] M. Mittal, M. Sharma, O.P. Pandey, UV–Visible light induced photocatalytic studies of Cu doped ZnO NPs prepared by co-precipitation method, Sol. Energy, 110 (2014) 386–397.
[28] S.R. Shirsath, D.V. Pinjari, P.R. Gogate, S.H. Sonawane, A.B. Pandit, Ultrasound assisted synthesis of doped TiO_2 nanoparticles: characterization and comparison of effectiveness for photocatalytic oxidation of dyestuff effluent, Ultrason. Sonochem., 20 (2013) 277–286.
[29] S. Aghabeygi, L. Hashemi, A. Morsali, Synthesis and characterization of ZnO nano-rods via thermal decomposition of zinc(II) coordination polymers and their photocatalytic properties, J. Inorg. Organomet. Polym., 26 (2016) 495–499.
[30] L. Curkovic, D. Ljubas, H. Juretic, Photocatalytic decolorization kinetics of diazo dye Congo red aqueous solution by UV/TiO_2 nanoparticles, React. Kinet. Mech. Catal., 99 (2010) 201–208.
[31] M.H. Habibi, M.H. Rahmati, The effect of operational parameters on the photocatalytic degradation of Congo red organic dye using ZnO–CdS core–shell nano-structure coated on glass by Doctor Blade method, Spectrochim. Acta, 137 (2015) 160–164.
[32] T. Linda, S. Muthupoongodi, X.S. Shajan, S. Balakumar, Photocatalytic degradation of Congo red and crystal violet dyes on cellulose/PVC/ZnO composites under UV light irradiation, Mater. Today, 3 (2016) 2035–2041.
[33] L. Ren, Y. Li, J. Hou, X. Zhao, C. Pan, Preparation and enhanced photocatalytic activity of TiO_2 nanocrystals with internal pores, ACS. Appl. Mater. Inter., 6 (2014) 1608–1615.
[34] G.R. Dillip, T.V.M. Sreekanth, S.W. Joo, Tailoring the bandgap of N-rich graphitic carbon nitride for enhanced photocatalytic activity, Ceram. Int., 43 (2017) 6437–6445.
[35] S.V.P. Vattikuti, I.L. Ngo, C. Byon, Physicochemcial characteristic of CdS-anchored porous WS2 hybrid in the photocatalytic degradation of crystal violet under UV and visible light irradiation, Solid State Sci., 61 (2016) 121–130.
[36] Y.L. Pang, A.Z. Abdullah, Comparative study on the process behavior and reaction kinetics in sonocatalytic degradation of organic dyes by powder and nanotubes TiO_2, Ultrason. Sonochem., 19 (2012) 642–651.
[37] A. Khan, Z. Rehman, M. Rehman, R. Khan, Zulfiqar, A. Waseem, A. Iqbal, Z.H. Shah, CdS nanocapsules and nanospheres as efficient solar light-driven photocatalysts for degradation of Congo red dye, Inorg. Chem. Commun., 72 (2016) 33–41.
[38] Y.J. Lin, M.S. Wang, C.J. Liu, H.J. Huang, Defects, stress and abnormal shift of the (002) diffraction peak for Li-doped ZnO films, Appl. Surf. Sci., 256 (2010) 7723–7727.